

Potassium Ion Selective Electrode Using Polyaniline and Matrix-Supported Ion-Selective PVC Membrane

Thuy Nguyen Thanh Tran, Shide Qiu, and Hyun-Joong Chung^{ID}

Abstract—Solid-state potassium ion selective electrode (K^+ ISE) has been the most studied chemical sensors due to its practical importance in biomedical applications. One of the major obstacles that prevented widespread use of solid-state K^+ ISE has been output potential drift problem. In this paper, we developed an electrochemical sensing unit in which working, counter, and reference electrodes are integrated in a single plane as all-solid-state form. In order to mitigate the output potential drift, a polyaniline intermediate layer and salt-saturated polyvinylbutyral top coating are introduced in the working and reference electrodes, respectively. Using cyclic voltammetry (CV), uniform layers of polyaniline are deposited on carbon electrode, as confirmed by scanning electron microscope observation. Potentiometry and electrochemical impedance spectroscopy measurement on our K^+ ISE show high sensitivity (60.5 mV/decade), low concentration for the limit of detection ($10^{-5.8}$ M), and large range of linear detection (10^{-5} – 1 M), and superior selectivity of K^+ ISE against NH_4^+ , Na^+ , Mg^{2+} , Ca^{2+} , and Fe^{3+} . With its high potential to be miniaturized, we foresee that our solid-state K^+ ISE will motivate the future applications in microdevices for clinical analysis, agricultural, and environmental applications.

Index Terms—Solid-state ion selective electrode, potassium sensor, potentiometry, signal stability.

I. INTRODUCTION

WEARABLE devices for health monitoring create new opportunities for personalized remote healthcare in recent years [1]. Chemical homeostasis is one of the most important subjects for sensors. Among chemicals, potassium ions have critical importance for all levels of vital activities [2]. In fact, potassium monitoring in food and serum [3], urine [4], and potentially in brain [5] has been a routine analysis in the clinical and medical fields to reveal physical conditions of the patients having renal diseases, hypopotassemia, alkalosis, cirrhosis of liver, or using diuretic drugs [6]. Thus, miniaturized K^+ sensor is highly demanded for wearable health monitoring system.

Conventional K^+ sensing methods include flame photometry [7]–[9], ion chromatography [10], surface

plasmon resonance [11], and electrochemical detection [12]. Among these technologies, electrochemical ion-selective electrode (ISE) has many advantages including fabrication simplicity, high selectivity towards a specific ion, fast response time, wide linear range, reproducibility and potential for miniaturization [13]. Using solid-state ISEs without internal filling solution provides a durable, flexible and portable ion sensor that can easily be miniaturized.

Ionophores, complex molecules that allow permeation of the K^+ ions while block others, is the key material for solid-state ion selective electrodes. The discovery of ionophore for K^+ detection was based on biological research which revealed that valinomycin, a dodecadepsipeptide antibiotic which can be isolated from *Streptomyces*, possesses an internal cavity whose size matches closely with the diameter of K^+ [14]. This means that valinomycin can easily form ionic bonds with K^+ . Other ions, for example Na^+ , whose diameter is significantly smaller than the pore, cannot form a complex together; the selectivity for K^+ over Na^+ is over 1000 times [15]–[17]. The mobility of ionophore and lipophilic counterions in the ion selective membrane significantly affect the frequency of interaction of K^+ and ionophore at the polymer/solution interface, which is important for the functionality of ISE. Due to concentration gradient, K^+ that formed ionic bonding with ionophores are mobile inside the liquid phase (plasticizer) of ion selective membrane, while other species are blocked outside. In rigid polyvinyl chloride (PVC), diffusion coefficient was in range of 10^{-6} cm^2/s for small gas molecules such as H_2 and He, and up to 10^{-17} cm^2/s for CCl_4 , let alone bulky organic molecules such as valinomycin [18]. Hence, adding plasticizer to PVC membrane is necessary to promote diffusion process of ionophore and to equilibrate the chemical potential more quickly. This way, response time is shortened. Diffusion coefficient of valinomycin through membrane consisting of about 33% PVC - bis(2-ethylhexyl) sebacate (DOS) is in the order of 10^{-8} cm^2/s [19].

Figure 1a illustrates the mechanism that causes the issue of potential instability when the ion selective membrane is in direct contact with the electron-conducting substrate. According to the Nernst equation, membrane potential changes logarithmically to K^+ ions activity; this can only be true when $[K^+]$ transduces to the electric potential without any delay or loss [20]. Here, water layer at the interface between the ion selective membrane and electrically conducting substrate damps out capacitive junction and as a result, no tran-

Manuscript received July 3, 2018; revised August 20, 2018; accepted September 7, 2018. Date of publication September 20, 2018; date of current version October 23, 2018. This work was supported in part by NSERC and in part by CIHR. The associate editor coordinating the review of this paper and approving it for publication was Dr. Chang-Soo Kim. (Corresponding author: Hyun-Joong Chung.)

The authors are with the Department of Chemical and Materials Engineering, Faculty of Engineering, University of Alberta, Edmonton, AB T6G 1H9, Canada (e-mail: chung.hj13@ualberta.ca).

Digital Object Identifier 10.1109/JSEN.2018.2871001

TABLE I
SUMMARY OF RECENT STUDIES OF SOLID-STATE POTASSIUM ION SELECTIVE ELECTRODES

Electrode	Intermediate layer/ Ionophore	Reference	Selectivity ($-\log K_{K^+, Na^+}$)	Sensitivity (mV/decade)	LOD (10^{-n} M)	Linear range (M)	Ref.
GC	N/A / valinomycin	SCE	N/A	49	5	$10^{-5} - 10^{-1}$	[32]
Pt	Ppy / calixarene	N/A	N/A	51	5.7	$10^{-5.2} - 10^{-1}$	[33]
Pt	PANI / dbdb-18-6	SCE	2.5	58	5.8	$10^{-5} - 10^{-1}$	[27]
Au	PEDOT-PSS / valinomycin	Ag/AgCl/3 M KCl	3	61.3	3	$10^{-3} - 10^{-1.5}$	[34]
GC	Graphene / valinomycin	N/A	N/A	58.4	6.2	$10^{-5.8} - 10^{-1}$	[35]
Graphite	Mixture of CB, poly(amidoacid) Cu(I) complex, resin / valinomycin	Ag/AgCl/3.5 M KCl	N/A	59	7	$10^{-6} - 10^{-1}$	[36]
Cu	Graphite-epoxy-hardener / valinomycin	Solid Ag/AgCl	4.11	44	4.4	$10^{-4.3} - 10^{-1}$	[37]
Ag	N/A / PBE	Ag/AgCl/3 M KCl	1.3	56.3	4.7	$10^{-4} - 10^{-1}$	[38]
GC	Hexanethiolate monolayer protected gold cluster / valinomycin	Ag/AgCl/3 M KCl	N/A	57.4	6.1	$10^{-5} - 10^{-1}$	[39]
Pt	Ppy and zeolite / valinomycin	Ag/AgCl/3 M KCl	N/A	54.2	5.1	$10^{-5} - 10^{-2}$	[12]
GC	MoO ₂ / valinomycin	Ag/AgCl/3 M KCl	N/A	55	5.5	$10^{-5} - 10^{-3}$	[40]
Carbon SPE	PANI / valinomycin	Modified solid Ag/AgCl	4.36	60.5	5.8	$10^{-5} - 1$	This work

LOD: limit of detection; GC: glassy carbon; N/A: not available; SCE: saturated calomel electrode; Pt: platinum; Ppy: polypyrrole; PANI: polyaniline; dbdb-8-6: 4',4''(5'')-di-tert-butylidibenzo-18-crown-6-ether; PEDOT-PSS: poly(3,4-ethylenedioxythiophene) polystyrene sulfonate; CB: carbon black; PBE: poly(benzyl eugenol); SPE: screen-printed electrode

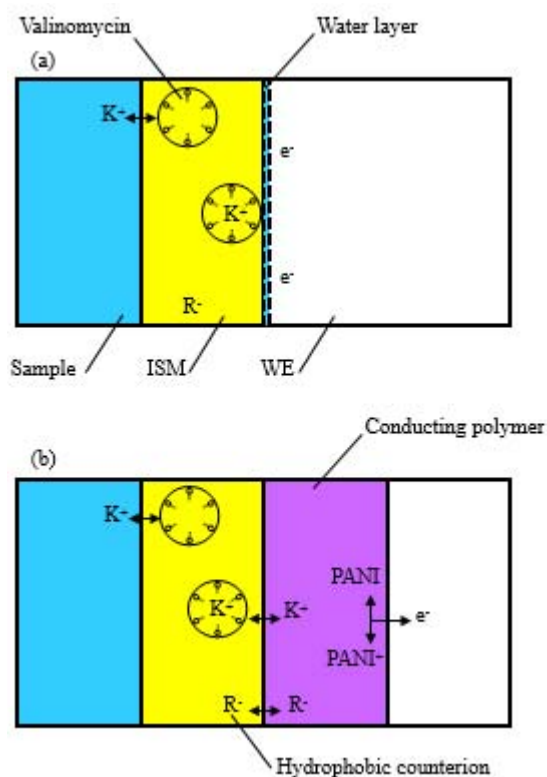


Fig. 1. Schematics that describe: (a) the water layer that forms between the ion selective membrane and electronically conducting substrate and (b) how an electrochemically transducing intermediate layer, such as polyaniline (PANI), mitigates the adverse effect by the water layer.

sition from ions to electrons [14]. In 2000, it has been proved that a thin water layer between Au and ion selective membrane is responsible for the potential drift and such problem can be reduced by depositing a lipophilic monolayer, such as thiol compounds, on top of the metal contact [21]. Alternatively,

conducting polymer between the electronic conductor and the ion-selective membrane to give high potential stability but does not influence the analytical performance of ISE including selectivity, sensitivity, and limit of detection [20]. Over the past few years, conducting polymers have been applied as promising ion-to-electron transducers for solid contact ISEs because they exhibit both electrical and ionic conductivity which means they can help ion-to-electron transition by oxidation/reduction of conducting polymers (Figure 1b) [22], [23]. Many electronically conducting polymers including polypyrroles [24], poly(3-octylthiophene) (POT) [25], and poly(3,4-ethylene-dioxythiophene) (PEDOT) [26], and polyaniline (PANI) [27] were tested as ion-to-electron transducers. It should be noted that PANI does not prevent water layer formation; rather, its conductivity is stable over a wide range of water content [28], [29]. Therefore, in this study, PANI was chosen due to its high conductivity in presence of water ($10^{-3} - 10^{-2}$ S/cm) and facile synthesis.

With an emergence of flexible and wearable bioelectronics, there has been a revival of ion selective electrodes in the last few years owing to its potential to miniaturization. This novel application requires a complete integrated system of ISE and reference electrode. Most of the recent studies solely focus on the modifications of WE while the effect of RE modification is less frequently studied (see Table 1 and references therein). In fact, the stability of miniaturized RE has been a longstanding issue for potentiometric measurements using solid-state electrodes [21], [30]. The purpose of a RE is to provide a stable potential that is independent with surrounding sample. The major issue of solid-state Ag/AgCl RE was the leakage of inorganic salt [31]. In this study, we employed the NaCl-saturated PVB membrane to prevent the leakage of AgCl; the aim of our work was to come up with a simple method to fabricate a K⁺ ISE with high selectivity and stable sensitivity. We applied a commercial

screen-printed electrode (SPE) with an extra intermediate layer (polyaniline) to solve the potential drift problem. Additionally, the miniaturized reference electrode (Ag/AgCl) was placed on the same plane as working electrode and was modified by polyvinyl butyral (PVB) and sodium chloride layer to maintain constant concentration of chloride ions and prevent leaking of silver chloride. Finally, our K^+ ISE exhibits good selectivity ($-\log K_{K^+, Na^+} = 4.36$), high sensitivity (60.5 mV/decade), low concentration for the limit of detection ($10^{-5.8}$ M), large range of linear detection ($10^{-5} - 1$ M), and potential stability (up to 12 hours) high concentration of NaCl mimics the salt bridge, thus the output stability was further enhanced.

II. MATERIALS AND METHODS

A. Materials and Instruments

Aniline, potassium ionophore I (Valinomycin), potassium tetrakis(4-chlorophenyl)borate (KTCBP), bis(2-ethylhexyl) sebacate (DOS), high molecular weight poly(vinyl chloride) (PVC), tetrahydrofuran (THF), potassium chloride (KCl), sodium chloride (NaCl), polyvinyl butyral (PVB, Butvar®B-98), methanol (CH_3OH), ammonium chloride (NH_4Cl) and Iron(III) chloride ($FeCl_3$) were purchased from Sigma-Aldrich. Hydrochloric acid was purchased from Caledon Laboratories Ltd. Magnesium chloride ($MgCl_2$) and calcium chloride ($CaCl_2$) were purchased from Fisher Scientific. All the chemicals were of analytical grade and used as received without further purification. Artificial blood serum (pH 7.4) was prepared by adding 0.05 mM NH_4Cl , 130 mM NaCl, 0.8 $MgCl_2$, and 1.4 mM $CaCl_2$ in de-ionized water (DIW).

Morphology of polyaniline was observed by field-emission scanning electron microscope (Zeiss EVO MA10, Jena, Germany). Electrochemical measurements were carried out with AUTOLAB potentiostat/galvanostat (PGSTAT302N, Metrohm Autolab B.V., Utrecht, The Netherlands). Commercial screen-printed electrodes (DRP 150, DropSense, S.L., Llanera, Spain) containing a carbon working electrode (diameter: 4 mm), a solid Ag/AgCl reference electrode and a platinum counter electrode were used to prepare K^+ ISE. All the experiments were conducted at room temperature (20°C).

B. PANI Polymerization

Carbon working electrode on SPE was coated with PANI by using cyclic voltammetry from 0 to 1 V vs. Ag/AgCl with scan rate of 100 mV/s in 0.03 M aniline and 0.05 M HCl. The process was repeated 30 cycles and stopped at 1 V. Here, we denote the PANI coated SPE as SPE/PANI. After that, SPE/PANI was dried in oven for 30 mins at 110°C. After that, SPE/PANI was inserted 0.1 M KCl and cyclic voltammetry from -0.5 to 1 V vs. Ag/AgCl with scan rate of 100 mV/s was performed to characterize PANI layer.

C. Preparation of K^+ Ion Selective Electrode

Ion selective membrane (ISM) cocktail used in this work consists 2% valinomycin, 0.6% KTCBP, 64.7% DOS, and 32.7% PVC (w/w%). Then, 100 mg of the mixture was

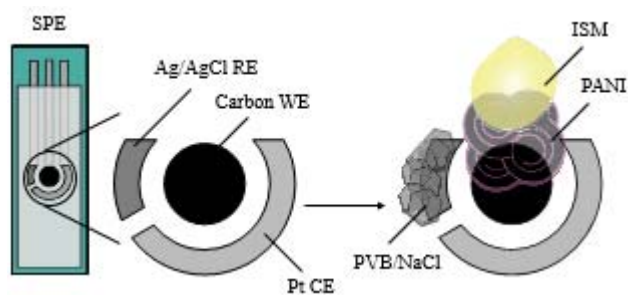


Fig. 2. The modified electrode configuration of solid contact K^+ ISE (ion selective electrode).

dissolved in 1 mL THF. As shown in Figure 2, 10 μL of the valinomycin-containing solution was deposited on SPE/PANI and let dry at room temperature overnight. Here, we denote the trilayer working electrode as SPE/PANI/V. A control sample to study the efficacy of the PANI intermediate layer was also prepared by drop casting the ISM cocktail on the bare SPE without PANI layer; we denote this sample as SPE/V. In addition, solution for reference electrode was made of 79.1 mg PVB and 50 mg NaCl in 1 mL methanol. Drop cast 3 μL of this solution onto Ag/AgCl reference electrode.

D. Electromotive Force Measurements (EMF)

Prepared electrodes (SPE/V and SPE/PANI/V) were conditioned in 0.01 M KCl solution for 2 h prior to use. The selectivity factors were determined by separate solution method to measure EMF of different solutions of K^+ , NH_4^+ , Na^+ , Mg^{2+} , Ca^{2+} , Fe^{3+} at the same activity (0.1 M).

Sensitivity of K^+ ISE was determined by measuring in diluted KCl solution through 8 concentration steps (1, 10^{-1} , 10^{-2} , 10^{-3} , 10^{-4} , 10^{-5} , 10^{-6} , 10^{-7} M KCl). After measuring the electrode in a solution for 120 seconds, the electrode was quickly cleaned with DIW and immersed in the next solution. Similarly, response of K^+ ISE was measured in artificial serum with spiked KCl between 10^{-5} and 1 M.

E. Electrochemical Impedance Spectroscopy (EIS)

EIS was measured with SPE/V, SPE/PANI/V and SPE/PANI/V without modified reference electrode. Impedance spectra were recorded in the frequency range 100 kHz to 10 mHz at the open circuit potential in 0.1 M KCl. The modulation amplitude used was 10 mV. Data was fitted based on the equivalent circuit models in ZSimpWin software to elucidate electrochemical process between the interface of solution and electrode.

F. Potential Stability Measurements

Potential was performed for SPE/PANI/V with and without PVB/NaCl layer on reference electrode in 0.1 M of KCl for 12 hours.

III. RESULTS AND DISCUSSION

A. Characterization of Polyaniline

In general, electrochemical polymerisation of aniline can be carried out by using one of the three techniques:

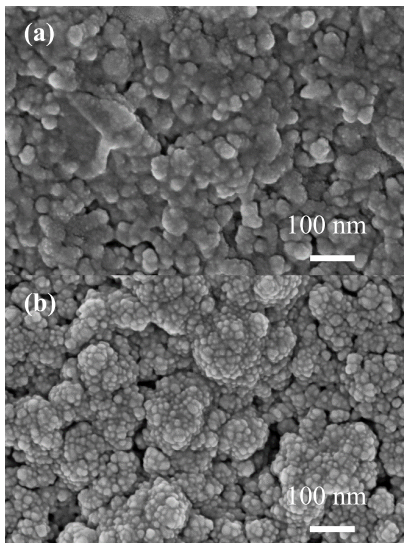


Fig. 3. SEM images showing morphology of (a) SPE (the bare carbon working electrode) and (b) SPE/PANI (PANI deposited on carbon working electrode by 30 CV cycles).

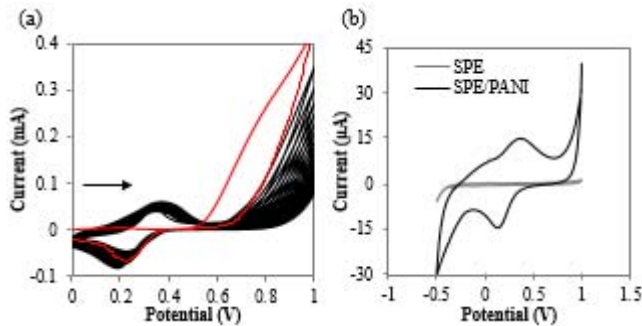


Fig. 4. Cyclic voltammetry (CV) spectra that were obtained (a) during the deposition of PANI in 0.5 M HCl (30 cycles overlapped; red line shows the first scan) and (b) after the 30-cycle deposition of PANI in 0.1 M KCl for quality evaluation (third scan). Here in (b), the spectrum from pure SPE was also overlaid for comparison.

(i) potentiostatic method (applying a constant voltage), (ii) cyclic voltammetry (CV), and (iii) galvanostatic method (applying a constant current) to an aqueous solution of aniline. PANI was deposited on WE as described in the experimental section by using CV. Here, we adopted the CV method for PANI deposition because it allows a more homogeneous deposition [41]. We found that 30 cycles allowed the best result for PANI layer quality, in terms of the balance between thickness and adhesion. Figure 3 shows the morphological contrast between SPE and SPE/PANI. Here, we confirmed that the 30 CV cycles allow well-distributed granular PANI homogeneously deposited on the carbon electrode.

Figure 4a shows the polymerization of aniline in 0.5 M HCl. The wide oxidation peak in the first cycle at 0.8 V vs. Ag/AgCl reflects the nucleation of aniline onto the site of carbon. After the first scan, this oxidation peak decreases and well-defined new peaks at 0.2 and 0.35 V indicate the growth of PANI film [42]. After the polymerization step, electrode was inserted into a solution of 0.1 M KCl to evaluate the quality of the formed polymer layer. In Figure 4b, the redox peaks

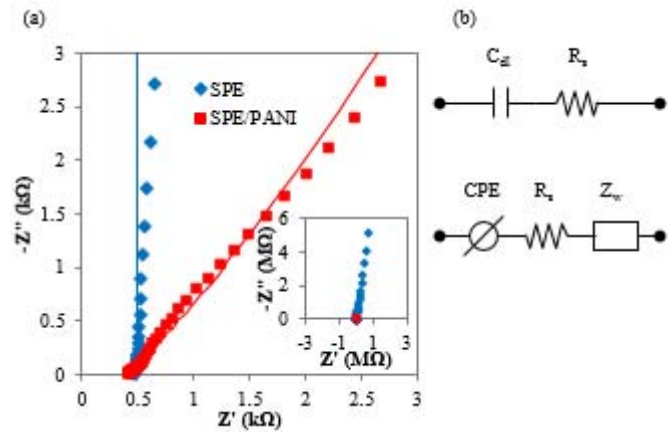


Fig. 5. (a) Electrochemical impedance spectroscopy (EIS) spectrum at high frequency of WE before and after aniline polymerization in 0.1 M KCl. Dot results were obtained from experiments while straight line represented fitting data from ZSimpWin. Inset plot shows full EIS spectrum. (b) The two equivalent circuits to fit SPE (top) and SPE/PANI (bottom).

at 0.130 and 0.370 are assigned to the reduction of partly oxidized emeraldine (electrically conducting) to the reduced form leucoemeraldine (electrically insulating) and vice versa. The produced PANI varies with oxidation states ranging from leucoemeraldine (fully reduced), emeraldine (half oxidized), and pernigraniline (fully oxidized) [43]. The CV result in Fig 4a indicates that some portion of the produced PANI is leucoemeraldine, which has the worst electrical conductivity among PANI ($10^{-10} - 10^{-8}$ S/cm) states. Fortunately, leucoemeraldine is very unstable and can easily be converted to emeraldine salt, which is electrically conducting ($10^{-2} - 10^{-1}$ S/cm), when dipped in an acidic medium [44], [45].

Figure 5a shows a Nyquist plot from EIS measurements of bare SPE and SPE/PANI in 0.1 M KCl solution with a modulation amplitude of 10 mV and the corresponding simulation results in line. Here, the imaginary axis for bare SPE is nearly perpendicular with real axis. Thus, the spectrum of the bare SPE can be fitted to a series circuit of solution resistance (R_s) and double layer capacitance (C_{dl}). On the other hand, that the spectrum of SPE/PANI inclines outward. In this case, a series of solution resistance (R_s), a constant phase element (CPE), and Warburg impedance (Z_w). CPE is a fitting parameter in electrochemical impedance measurements to represent an imperfect capacitor. There are many factors that causes a CPE such as surface roughness, varying thickness or pore size distribution across electrode surface resulting in inhomogeneous reaction rate [46], [47]. The adoption of CPE in the equivalent circuit for SPE/PANI is reasonable because PANI deposited on electrode surface increases electrode surface roughness and homogeneity.

B. Selectivity Test

Selectivity coefficient K_{ij}^{pot} one of the most important parameter to determine the quality of an ISE. The selectivity is determined by combination of ionophore and other electrode membrane components. Here, Nernst equation for real

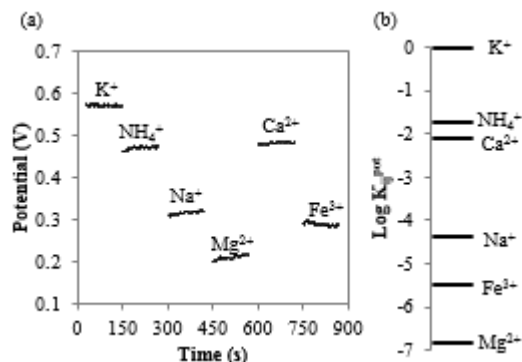


Fig. 6. Response of K^+ ISE for different cations at the same activity (0.1 M). (a) Potential values from potentiometry measurement and (b) selectivity coefficient K_{ij}^{pot} calculated from (a).

solutions presenting ion of interest i and interfering species j is:

$$E = E^0 + \frac{RT}{z_i F} \ln \left(a_i + \sum K_{ij}^{pot} (a_j)^{z_i/z_j} \right) \quad (1)$$

with E : electrode potential, E^0 : standard electrode potential, R : gas constant, T : absolute temperature, z : valence of the ion, F : Faraday constant, and a : activity of the ion.

In our study, we employed a separate solution method to measure selectivity coefficient K_{ij}^{pot} [48]. The potential of SPE/PANI/V is measured with separate solutions of cations at the same activity (0.1 M). If the measured values are E_i and E_j for K^+ and other interferents, respectively, the value of K_{ij}^{pot} may be calculated from the equation:

$$\log K_{ij}^{pot} = \frac{(E_j - E_i) z_i F}{RT \ln 10} + \left(1 - \frac{z_i}{z_j} \right) \log a_i \quad (2)$$

As shown in Figure 6, K_{ij}^{pot} was obtained for mono-, di- and trivalent cations. NH_4^+ can interfere the most with K^+ detection because NH_4^+ has a similar value of hydrated ionic radius as K^+ ion. In case of biomedical applications such as analyzing human's interstitial fluid, Na^+ and K^+ are of the most concern. Here, $[Na^+]$ typically varies between 145 – 155 mM while K^+ level fluctuates between 3.5 – 5.5 mM [49]. Our sensing electrode displayed K_{ij}^{pot} value of Na^+ over K^+ to be about 4.32×10^{-5} , meaning it takes more than 23,000 Na^+ ions to modulate the electrode potential as one K^+ ion does. Therefore, the selectivity of our electrode is adequate to apply in analyzing human's interstitial fluid.

C. Sensitivity Test

Figure 7a shows the potential output between the working and the reference electrodes when SPE/V and SPE/PANI/V were employed as working electrodes, respectively, with respect to time immersed in the KCl solution with varying ionic concentration. The figure also evidences that the inclusion of PANI interlayer remarkably reduces the potential drift. Constructing a calibration curve (i.e. replotting the average potential values against $[K^+]$) in Figure 7b shows that SPE/V and SPE/PANI/V have a linear range

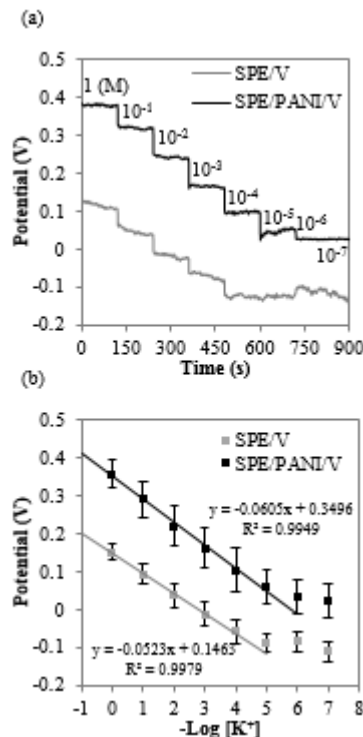


Fig. 7. (a) Electromotive force (EMF) measurements recorded for decreasing concentration of K^+ in DIW, (b) average calibration curve ($N = 3$).

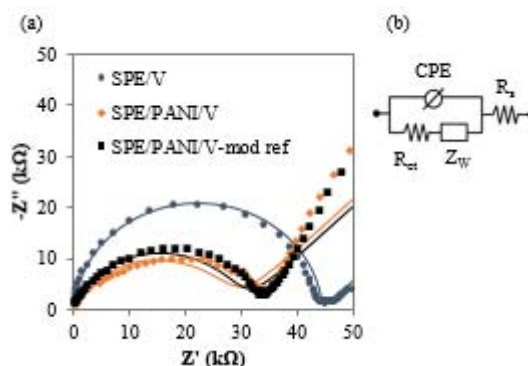


Fig. 8. (a) Impedance measurements between SPE/V, SPE/PANI/V (with as-received reference electrode), and SPE/PANI/V with PVB modified reference electrode. (b) The equivalent circuit used for simulations to fit the measured EIS spectra.

from 10^{-4} to 1 M and 10^{-5} to 1 M of KCl, respectively. As a result, detection limit was improved from $10^{-4.3}$ M (SPE/V) to $10^{-5.8}$ M (SPE/PANI/V) of KCl, and sensitivity increased from 52.3 ± 3.1 mV/decade (SPE/V) to 60.5 ± 5.3 mV/decade (SPE/PANI/V).

D. EIS

In this part, EIS measurements were fitted to the equivalent circuit (Figure 8b) representing solution resistance (R_s), charge transfer resistance (R_{ct}) at the membrane/solution interface, CPE and the finite-length Warburg impedance (Z_W). As mentioned before, CPE was used instead of capacitor for better agreement with the measurement. We intended to make

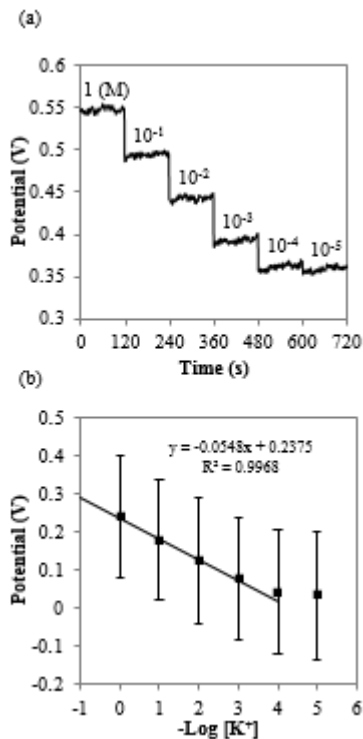


Fig. 9. (a) EMF measurements recorded for decreasing concentration of K^+ in artificial serum, (b) average calibration curve ($N = 3$).

observation whether there is a qualitative difference between the three differently modified electrodes, SPE/V, SPE/PANI/V, and SPE/PANI/V with PVB modified reference electrodes. As can be seen in Figure 8a, smaller semicircle indicates the reduction in charge transfer resistance of SPE/PANI/V compared to SPE/V. In addition, the PVB modification on RE did not impact the characteristics of K^+ ISE.

E. Artificial Serum Test

Ion fluxes are highly regulated across human cell membrane by specific ion channels; especially crucial for signaling in nerve and muscle cells are K^+ of which intracellular and extracellular concentration exhibit the utmost level of selective control between 130 – 150 and 3.5 – 5.5 mM, respectively [50]–[52]. Any disequilibrium implies neuronal diseases (*i.e.* epilepsy) or nephrosis (*i.e.* renal failure), where K^+ concentration in extracellular space reaches up to 10 mM may cause a stroke [27], [52]. Extracellular fluids (blood plasma and interstitial fluid) contains various analytes from cations, anions, organic acids and proteins. Figure 9 has shown that, in artificial blood serum, K^+ ISE still gives a good linear result covering from 10^{-3} to 1 M with 54.8 ± 1.2 mV/decade, and detection limit of $10^{-3.5}$ M of KCl, which is well below the normal level in human extracellular fluids.

F. Potential Stability

This test is carried out to evaluate the stability of K^+ ISE when reference electrode is covered with PVB/NaCl layer. Solid Ag/AgCl reference is unstable due to delamination

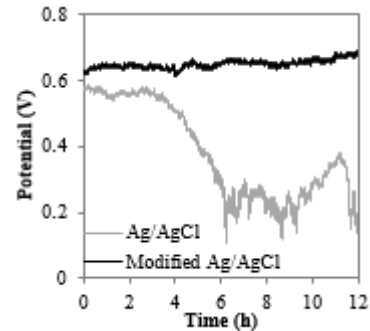


Fig. 10. EMF measurements in 0.1 M KCl of K^+ ISE with and without PVB/NaCl layer on reference electrode.

of AgCl salt in aqueous solution. As shown in Figure 10, potential drift of K^+ electrode vs. Ag/AgCl was calculated by measuring the slope of potential in the first 3 hours to be $1.17 \mu\text{V/s}$, followed by severe instability. On the other hand, the potential drift of K^+ electrode vs. modified Ag/AgCl was $0.78 \mu\text{V/s}$ in 12 hours, while the signal stayed stable and consistent over the entire duration of the measurement. Therefore, PVB/NaCl membrane has proved to prevent leaking of AgCl.

IV. CONCLUSION

In this study, PANI has proved to enhance the performance of potassium sensor whose sensitivity was 60.5 mV/decade. Limit of detection for potassium ions was $10^{-5.8}$ M. In addition, modified solid Ag/AgCl reference prolongs the stability of output potential. PANI based potassium ion selective electrodes and PVB/NaCl coated reference electrodes have been tested in artificial serum. The demonstrated high sensitivity, short-term stability and all-in-one solid-state setup may add another stepping stone towards biomedical applications for monitoring the concentration of K^+ in important healthcare applications, such as blood, plasma, serum, sweat in future studies.

REFERENCES

- [1] X. Wang, Z. Liu, and T. Zhang, "Flexible sensing electronics for wearable/attachable health monitoring," *Small*, vol. 13, no. 25, p. 1602790, 2017.
- [2] B. F. Palmer, "Regulation of potassium homeostasis," *Clin. J. Amer. Soc. Nephrol.*, vol. 10, no. 6, pp. 1050–1060, 2015.
- [3] S. Komaba, J. Arakawa, M. Seyama, T. Osaka, I. Satoh, and S. Nakamura, "Flow injection analysis of potassium using an all-solid-state potassium-selective electrode as a detector," *Talanta*, vol. 46, no. 6, pp. 1293–1297, 1998.
- [4] T. Zhang *et al.*, "Comparison of sodium, potassium, calcium, magnesium, zinc, copper and iron concentrations of elements in 24-h urine and spot urine in hypertensive patients with healthy renal function," *J. Trace Elements Med. Biol.*, vol. 44, pp. 104–108, Dec. 2017.
- [5] M. Odijk *et al.*, "Microfabricated solid-state ion-selective electrode probe for measuring potassium in the living rodent brain: Compatibility with DC-EEG recordings to study spreading depression," *Sens. Actuators B, Chem.*, vol. 207, pp. 945–953, Feb. 2015.
- [6] A. S. Lima, N. Bocchi, H. M. Gomes, and M. F. Teixeira, "An electrochemical sensor based on nanostructured hollandite-type manganese oxide for detection of potassium ions," *Sensors*, vol. 9, no. 9, pp. 6613–6625, 2009.
- [7] R. D. Amrutkar, A. E. Thube, and S. C. Kulkarni, "Determination of sodium and potassium content present in water sample collected from Girna and Godavari river by flame photometry," *J. Pharmaceutical Sci. Biosci. Res.* vol. 3, no. 3, pp. 105–107, 2013.

- [8] I. S. El Otmani *et al.*, "Correlation study between two analytical techniques used to measure serum potassium: An automated potentiometric method and flame photometry reference method," *J. Chem. Pharmaceutical Res.*, vol. 7, no. 8, pp. 862–867, 2015.
- [9] V. Albert, A. Subramanian, K. Rangarajan, and R. M. Pandey, "Agreement of two different laboratory methods used to measure electrolytes," *J. Lab. Phys.*, vol. 3, no. 2, pp. 104–109, 2011.
- [10] B. S. Yu, L. H. Nie, and S. Z. Yao, "Ion chromatographic study of sodium, potassium and ammonium in human body fluids with bulk acoustic wave detection," *J. Chromatogr. B, Biomed. Sci. Appl.*, vol. 693, no. 1, pp. 43–49, 1997.
- [11] H. Chen *et al.*, "Potassium ion sensing using a self-assembled calix[4]crown monolayer by surface plasmon resonance," *Sens. Actuators B, Chem.*, vol. 133, no. 2, pp. 577–581, 2008.
- [12] K. Yu, N. He, N. Kumar, N. Wang, J. Bobacka, and A. Ivaska, "Electrosynthesized polypyrrole/zeolite composites as solid contact in potassium ion-selective electrode," *Electrochim. Acta*, vol. 228, pp. 66–75, Feb. 2017.
- [13] J. Bobacka, A. Ivaska, and A. Lewenstam, "Potentiometric ion sensors," *Chem. Rev.*, vol. 108, no. 2, pp. 329–351, 2008.
- [14] L. van de Velde, E. D'Angremont, and W. Olthuis, "Solid contact potassium selective electrodes for biomedical applications—A review," *Talanta*, vol. 160, pp. 56–65, Nov. 2016.
- [15] H. Beyer and W. Walter, *Organic Chemistry: A Comprehensive Degree Text and Source Book*. Sawston, U.K.: Woodhead Publishing, 1997.
- [16] C. J. Jones and J. R. Thornback, "Macrocyclic antibiotics," in *Medicinal Applications of Coordination Chemistry*. Cambridge, U.K.: Royal Society of Chemistry, 2007.
- [17] W. Steglich, B. Fugmann, and S. Lang-Fugmann, *Römpp Encyclopedia Natural Products*. Stuttgart, Germany: Thieme Medical Publishers, 2001.
- [18] A. R. Berens, "Solubility and diffusion of small molecules in PVC," *J. Vinyl Technol.*, vol. 11, no. 4, pp. 171–175, 1989.
- [19] G. Harsanyi, *Polymer Films in Sensor Applications*. Boca Raton, FL, USA: CRC Press, 1995, p. 464.
- [20] J. Bobacka and A. Ivaska, "Ion sensors with conducting polymers as ion-to-electron transducers," in *Comprehensive Analytical Chemistry*, vol. 49. Amsterdam, The Netherlands: Elsevier, 2007, ch. 4, pp. 73–86.
- [21] M. Fibioli, W. E. Morf, M. Badertscher, N. F. de Rooij, and E. Pretsch, "Potential drifts of solid-contacted ion-selective electrodes due to zero-current ion fluxes through the sensor membrane," *Electroanalysis*, vol. 12, no. 16, pp. 1286–1292, 2000.
- [22] J. Bobacka, "Conducting polymer-based solid-state ion-selective electrodes," *Electroanalysis*, vol. 18, no. 1, pp. 7–18, 2006.
- [23] A. Michalska, "Optimizing the analytical performance and construction of ion-selective electrodes with conducting polymer-based ion-to-electron transducers," *Anal. Bioanal. Chem.*, vol. 384, no. 2, pp. 391–406, 2006.
- [24] R. Mamińska and W. Wróblewski, "Solid-state microelectrodes for flow-cell analysis based on planar back-side contact transducers," *Electroanalysis*, vol. 18, nos. 13–14, pp. 1347–1353, 2006.
- [25] J. P. Veder *et al.*, "Evidence for a surface confined ion-to-electron transduction reaction in solid-contact ion-selective electrodes based on poly(3-octylthiophene)," *Anal. Chem.*, vol. 85, no. 21, pp. 10495–10502, 2013.
- [26] J. Bobacka, "Potential stability of all-solid-state ion-selective electrodes using conducting polymers as ion-to-electron transducers," *Anal. Chem.*, vol. 71, no. 21, pp. 4932–4937, 1999.
- [27] W.-S. Han, Y.-H. Lee, K.-J. Jung, S.-Y. Ly, T.-K. Hong, and M.-H. Kim, "Potassium ion-selective polyaniline solid-contact electrodes based on 4',4'(5')-di-tert-butylidibenzo-18-crown-6-ether ionophore," *J. Anal. Chem.*, vol. 63, no. 10, pp. 987–993, 2008.
- [28] S. C. Hobaica, "Stability of polyaniline in air and acidic water," *J. Polym. Sci. B, Polym. Phys.*, vol. 41, no. 8, pp. 807–822, 2003.
- [29] J. Luo, H. Zhang, X. Wang, J. Li, and F. Wang, "Stable aqueous dispersion of conducting polyaniline with high electrical conductivity," *Macromolecules*, vol. 40, no. 23, pp. 8132–8135, 2007.
- [30] J. Bobacka, A. Ivaska, and A. Lewenstam, "Potentiometric ion sensors based on conducting polymers," *Electroanalysis*, vol. 15, nos. 5–6, pp. 366–374, 2003.
- [31] J. Hu, A. Stein, and P. Bühlmann, "Rational design of all-solid-state ion-selective electrodes and reference electrodes," *TRAC Trends Anal. Chem.*, vol. 76, pp. 102–114, Feb. 2016.
- [32] J. Bobacka, A. Ivaska, and A. Lewenstam, "Plasticizer-free all-solid-state potassium-selective electrode based on poly(3-octylthiophene) and valinomycin," *Anal. Chim. Acta*, vol. 385, nos. 1–3, pp. 195–202, 1999.
- [33] N. Zine *et al.*, "Potassium-ion selective solid contact microelectrode based on a novel 1,3-(di-4-oxabutanol)-calix[4]arene-crown-5 neutral carrier," *Electrochim. Acta*, vol. 51, no. 24, pp. 5075–5079, 2006.
- [34] Z. Mousavi, J. Bobacka, A. Lewenstam, and A. Ivaska, "Poly(3,4-ethylenedioxythiophene) (PEDOT) doped with carbon nanotubes as ion-to-electron transducer in polymer membrane-based potassium ion-selective electrodes," *J. Electroanal. Chem.*, vol. 633, no. 1, pp. 246–252, 2009.
- [35] J. Ping, Y. Wang, J. Wu, and Y. Ying, "Development of an all-solid-state potassium ion-selective electrode using graphene as the solid-contact transducer," *Electrochem. Commun.*, vol. 13, no. 12, pp. 1529–1532, 2011.
- [36] N. M. Ivanova *et al.*, "Potassium-selective solid contact electrodes with poly(amidoacid) Cu(I) complex, electron-ion exchanging resin and different sorts of carbon black in the transducer layer," *Sens. Actuators B, Chem.*, vol. 186, pp. 589–596, Sep. 2013.
- [37] G. Vardar, M. Altıkatoğlu, D. Ortaç, M. Cemek, and I. İşildak, "Measuring calcium, potassium, and nitrate in plant nutrient solutions using ion-selective electrodes in hydroponic greenhouse of some vegetables," *Biotechnol. Appl. Biochem.*, vol. 62, no. 5, pp. 663–668, 2015.
- [38] D. Siswanta, Y. D. Wulandari, and J. Jumina, "Synthesis of poly(benzyleugenol) and its application as an ionophore for a potassium ion-selective electrode," *Eurasian J. Anal. Chem.*, vol. 11, no. 2, pp. 115–125, 2016.
- [39] Q. An *et al.*, "Robust single-piece all-solid-state potassium-selective electrode with monolayer-protected Au clusters," *J. Electroanal. Chem.*, vol. 781, pp. 272–277, Nov. 2016.
- [40] X. Zeng and W. Qin, "A solid-contact potassium-selective electrode with MoO₂ microspheres as ion-to-electron transducer," *Anal. Chim. Acta*, vol. 982, pp. 72–77, Aug. 2017.
- [41] Z. A. Boeva and V. G. Sergeev, "Polyaniline: Synthesis, properties, and application," *Polym. Sci. C*, vol. 56, no. 1, pp. 144–153, 2014.
- [42] C. P. Silva *et al.*, "Electrochemical transducer based on nanostructured polyaniline films obtained on functionalized self assembled monolayers of 4-aminothiophenol," *Mol. Cryst. Liq. Cryst.*, vol. 522, no. 1, pp. 112–124, 2010.
- [43] K. M. Molapo *et al.*, "Electronics of conjugated polymers (I): Polyaniline," *Int. J. Electrochem. Sci.*, vol. 7, no. 12, pp. 11859–11875, 2012.
- [44] N. Su, "Polyaniline-doped spherical polyelectrolyte brush nanocomposites with enhanced electrical conductivity, thermal stability, and solubility property," *Polymers*, vol. 7, no. 9, pp. 1599–1616, 2015.
- [45] I. Sapurina and J. Stejskal, "The mechanism of the oxidative polymerization of aniline and the formation of supramolecular polyaniline structures," *Polym. Int.*, vol. 57, no. 12, pp. 1295–1325, 2008.
- [46] R. De Levie, "The influence of surface roughness of solid electrodes on electrochemical measurements," *Electrochim. Acta*, vol. 10, no. 2, pp. 113–130, 1965.
- [47] H.-K. Song, H.-Y. Hwang, K.-H. Lee, and L. H. Dao, "The effect of pore size distribution on the frequency dispersion of porous electrodes," *Electrochim. Acta*, vol. 45, no. 14, pp. 2241–2257, 2000.
- [48] E. Bakker, E. Pretsch, and P. Bühlmann, "Selectivity of potentiometric ion sensors," *Anal. Chem.*, vol. 72, no. 6, pp. 1127–1133, 2000.
- [49] H. K. Walker, W. D. Hall, and J. W. Hurst, Eds., *Clinical Methods: The History, Physical and Laboratory Examinations*. Boston, MA, USA: Butterworth, 1990.
- [50] D. Kim, J. McCoy, and C. Nimgean, "Ion selectivity and conductance," in *Handbook of Ion Channels*. Boca Raton, FL, USA: CRC Press, 2015, pp. 13–23.
- [51] R. Chang and J. W. Thoman, "Electrochemistry," in *Physical Chemistry for the Chemical Sciences*. Mill Valley, CA, USA: Univ. Science Books, 2014.
- [52] A. Depauw *et al.*, "A highly selective potassium sensor for the detection of potassium in living tissues," *Chemistry*, vol. 22, no. 42, pp. 14902–14911, 2016.

Thuy Nguyen Thanh Tran, photograph and biography not available at the time of publication.

Shide Qiu, photograph and biography not available at the time of publication.

Hyun-Joong Chung, photograph and biography not available at the time of publication.